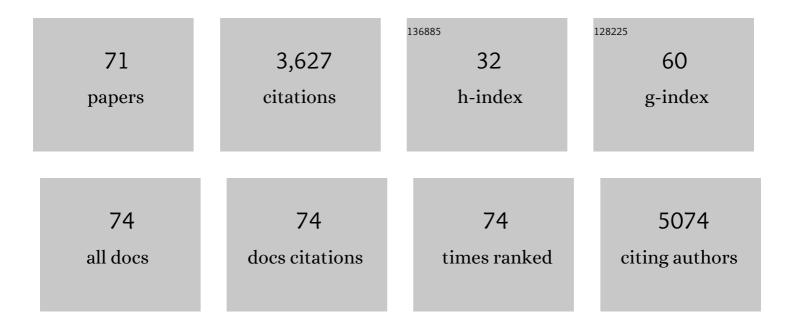
Ruichan Lv

List of Publications by Year in descending order

Source: https://exaly.com/author-pdf/5439773/publications.pdf Version: 2024-02-01



#	Article	IF	CITATIONS
1	A Yolk-like Multifunctional Platform for Multimodal Imaging and Synergistic Therapy Triggered by a Single Near-Infrared Light. ACS Nano, 2015, 9, 1630-1647.	7.3	319
2	Assembly of Au Plasmonic Photothermal Agent and Iron Oxide Nanoparticles on Ultrathin Black Phosphorus for Targeted Photothermal and Photodynamic Cancer Therapy. Advanced Functional Materials, 2017, 27, 1700371.	7.8	254
3	Integration of Upconversion Nanoparticles and Ultrathin Black Phosphorus for Efficient Photodynamic Theranostics under 808 nm Near-Infrared Light Irradiation. Chemistry of Materials, 2016, 28, 4724-4734.	3.2	193
4	An imaging-guided platform for synergistic photodynamic/photothermal/chemo-therapy with pH/temperature-responsive drug release. Biomaterials, 2015, 63, 115-127.	5.7	191
5	A New Single 808 nm NIR Lightâ€Induced Imagingâ€Guided Multifunctional Cancer Therapy Platform. Advanced Functional Materials, 2015, 25, 3966-3976.	7.8	178
6	g-C ₃ N ₄ Coated Upconversion Nanoparticles for 808 nm Near-Infrared Light Triggered Phototherapy and Multiple Imaging. Chemistry of Materials, 2016, 28, 7935-7946.	3.2	163
7	<i>In Situ</i> Growth Strategy to Integrate Up-Conversion Nanoparticles with Ultrasmall CuS for Photothermal Theranostics. ACS Nano, 2017, 11, 1064-1072.	7.3	132
8	A Single 808 nm Near-Infrared Light-Mediated Multiple Imaging and Photodynamic Therapy Based on Titania Coupled Upconversion Nanoparticles. Chemistry of Materials, 2015, 27, 7957-7968.	3.2	129
9	Multifunctional Anticancer Platform for Multimodal Imaging and Visible Light Driven Photodynamic/Photothermal Therapy. Chemistry of Materials, 2015, 27, 1751-1763.	3.2	109
10	Hyperthermia and Controllable Free Radical Coenhanced Synergistic Therapy in Hypoxia Enabled by Near-Infrared-II Light Irradiation. ACS Nano, 2019, 13, 13144-13160.	7.3	109
11	Controllable Generation of Free Radicals from Multifunctional Heat-Responsive Nanoplatform for Targeted Cancer Therapy. Chemistry of Materials, 2018, 30, 526-539.	3.2	103
12	Hollow Structured Y ₂ O ₃ :Yb/Er–Cu _{<i>x</i>} S Nanospheres with Controllable Size for Simultaneous Chemo/Photothermal Therapy and Bioimaging. Chemistry of Materials, 2015, 27, 483-496.	3.2	102
13	Au ₂₅ cluster functionalized metal–organic nanostructures for magnetically targeted photodynamic/photothermal therapy triggered by single wavelength 808 nm near-infrared light. Nanoscale, 2015, 7, 19568-19578.	2.8	99
14	Yolk-Structured Upconversion Nanoparticles with Biodegradable Silica Shell for FRET Sensing of Drug Release and Imaging-Guided Chemotherapy. Chemistry of Materials, 2017, 29, 7615-7628.	3.2	92
15	A core/shell/satellite anticancer platform for 808 NIR light-driven multimodal imaging and combined chemo-/photothermal therapy. Nanoscale, 2015, 7, 13747-13758.	2.8	78
16	Charge convertibility and near infrared photon co-enhanced cisplatin chemotherapy based on upconversion nanoplatform. Biomaterials, 2017, 130, 42-55.	5.7	77
17	Bismuth Nanoparticles with "Light―Property Served as a Multifunctional Probe for X-ray Computed Tomography and Fluorescence Imaging. Chemistry of Materials, 2018, 30, 3301-3307.	3.2	68
18	A Versatile Near Infrared Light Triggered Dual-Photosensitizer for Synchronous Bioimaging and Photodynamic Therapy. ACS Applied Materials & Interfaces, 2017, 9, 12993-13008.	4.0	66

Ruichan Lv

#	Article	IF	CITATIONS
19	Stable ICG-loaded upconversion nanoparticles: silica core/shell theranostic nanoplatform for dual-modal upconversion and photoacoustic imaging together with photothermal therapy. Scientific Reports, 2017, 7, 15753.	1.6	63
20	Highly Uniform Hollow GdF ₃ Spheres: Controllable Synthesis, Tuned Luminescence, and Drug-Release Properties. ACS Applied Materials & Interfaces, 2013, 5, 10806-10818.	4.0	55
21	Y ₂ O ₃ :Yb,Er@mSiO ₂ –Cu _x S double-shelled hollow spheres for enhanced chemo-/photothermal anti-cancer therapy and dual-modal imaging. Nanoscale, 2015, 7, 12180-12191.	2.8	55
22	A Novel double-shelled C@NiO hollow microsphere: Synthesis and application for electrochemical capacitor. Electrochimica Acta, 2014, 148, 211-219.	2.6	54
23	Black Phosphorus Nanosheet with High Thermal Conversion Efficiency for Photodynamic/Photothermal/Immunotherapy. ACS Biomaterials Science and Engineering, 2020, 6, 4940-4948.	2.6	52
24	Enhanced Upconversion Luminescence-Guided Synergistic Antitumor Therapy Based on Photodynamic Therapy and Immune Checkpoint Blockade. Chemistry of Materials, 2020, 32, 4627-4640.	3.2	50
25	Imaging-Guided and Light-Triggered Chemo-/Photodynamic/Photothermal Therapy Based on Gd (III) Chelated Mesoporous Silica Hybrid Spheres. ACS Biomaterials Science and Engineering, 2016, 2, 2058-2071.	2.6	46
26	Lutecium Fluoride Hollow Mesoporous Spheres with Enhanced Up-Conversion Luminescent Bioimaging and Light-Triggered Drug Release by Gold Nanocrystals. ACS Applied Materials & Interfaces, 2014, 6, 15550-15563.	4.0	42
27	Multifunctional SiO ₂ @Gd ₂ O ₃ :Yb/Tm Hollow Capsules: Controllable Synthesis and Drug Release Properties. Inorganic Chemistry, 2014, 53, 10917-10927.	1.9	41
28	Doxorubicin-conjugated CuS nanoparticles for efficient synergistic therapy triggered by near-infrared light. Dalton Transactions, 2016, 45, 5101-5110.	1.6	40
29	Nanochemistry advancing photon conversion in rare-earth nanostructures for theranostics. Coordination Chemistry Reviews, 2022, 460, 214486.	9.5	39
30	Surfactant-Free Synthesis, Luminescent Properties, and Drug-Release Properties of LaF ₃ and LaCO ₃ F Hollow Microspheres. Inorganic Chemistry, 2014, 53, 998-1008.	1.9	38
31	Coordination chemistry of the host matrices with dopant luminescent Ln3+ ion and their impact on luminescent properties. Coordination Chemistry Reviews, 2022, 466, 214584.	9.5	38
32	Dopamine-mediated photothermal theranostics combined with up-conversion platform under near infrared light. Scientific Reports, 2017, 7, 13562.	1.6	37
33	Design, fabrication, luminescence and biomedical applications of UCNPs@mSiO ₂ –ZnPc–CDs–P(NIPAm-MAA) nanocomposites. Journal of Materials Chemistry B, 2016, 4, 5883-5894.	2.9	35
34	CuS–Pt(<scp>iv</scp>)–PEG–FA nanoparticles for targeted photothermal and chemotherapy. Journal of Materials Chemistry B, 2016, 4, 5938-5946.	2.9	30
35	LaF ₃ :Ln mesoporous spheres: controllable synthesis, tunable luminescence and application for dual-modal chemo-/photo-thermal therapy. Nanoscale, 2014, 6, 14799-14809.	2.8	27
36	Peptide functionalized upconversion/NIR II luminescent nanoparticles for targeted imaging and therapy of oral squamous cell carcinoma. Biomaterials Science, 2021, 9, 1000-1007.	2.6	27

RUICHAN LV

#	Article	IF	CITATIONS
37	Degradable magnetic-response photoacoustic/up-conversion luminescence imaging-guided photodynamic/photothermal antitumor therapy. Biomaterials Science, 2019, 7, 4558-4567.	2.6	25
38	Markedly enhanced up-conversion luminescence by combining IR-808 dye sensitization and core–shell–shell structures. Dalton Transactions, 2017, 46, 1495-1501.	1.6	24
39	Highly Erbium-Doped Nanoplatform with Enhanced Red Emission for Dual-Modal Optical-Imaging-Guided Photodynamic Therapy. Inorganic Chemistry, 2018, 57, 14594-14602.	1.9	23
40	Targeted Luminescent Probes for Precise Upconversion/NIR II Luminescence Diagnosis of Lung Adenocarcinoma. Analytical Chemistry, 2021, 93, 4984-4992.	3.2	20
41	Self-produced bubble-template synthesis of La ₂ O ₃ :Yb/Er@Au hollow spheres with markedly enhanced luminescence and release properties. CrystEngComm, 2014, 16, 9612-9621.	1.3	17
42	Surface Plasmonic Enhanced Imaging-Guided Photothermal/Photodynamic Therapy Based on Lanthanide–Metal Nanocomposites under Single 808 nm Laser. ACS Biomaterials Science and Engineering, 2019, 5, 5051-5059.	2.6	17
43	When a Semiconductor Utilized as an NIR Laser-Responsive Photodynamic/Photothermal Theranostic Agent Integrates with Upconversion Nanoparticles. ACS Biomaterials Science and Engineering, 2019, 5, 3100-3110.	2.6	17
44	UCNPs@gelatin–ZnPc nanocomposite: synthesis, imaging and anticancer properties. Journal of Materials Chemistry B, 2016, 4, 4138-4146.	2.9	15
45	Improved Red Emission and Short-Wavelength Infrared Luminescence under 808 nm Laser for Tumor Theranostics. ACS Biomaterials Science and Engineering, 2019, 5, 4683-4691.	2.6	15
46	Degradable pH-responsive NIR-II imaging probes based on a polymer-lanthanide composite for chemotherapy. Dalton Transactions, 2020, 49, 9444-9453.	1.6	15
47	MET-targeted NIR II luminescence diagnosis and up-conversion guided photodynamic therapy for triple-negative breast cancer based on a lanthanide nanoprobe. Nanoscale, 2021, 13, 18125-18133.	2.8	15
48	Optimization of Red Luminescent Intensity in Eu ³⁺ -Doped Lanthanide Phosphors Using Genetic Algorithm. ACS Biomaterials Science and Engineering, 2018, 4, 4378-4384.	2.6	13
49	Multilevel Nanoarchitecture Exhibiting Biosensing for Cancer Diagnostics by Dual-Modal Switching of Optical and Magnetic Resonance Signals. ACS Applied Bio Materials, 2018, 1, 1505-1511.	2.3	13
50	Met-Targeted Dual-Modal MRI/NIR II Imaging for Specific Recognition of Head and Neck Squamous Cell Carcinoma. ACS Biomaterials Science and Engineering, 2021, 7, 1640-1650.	2.6	13
51	Up-Conversion Luminescence Properties of Lanthanide-Gold Hybrid Nanoparticles as Analyzed with Discrete Dipole Approximation. Nanomaterials, 2018, 8, 989.	1.9	12
52	Searching for the Optimized Luminescent Lanthanide Phosphor Using Heuristic Algorithms. Inorganic Chemistry, 2019, 58, 6458-6466.	1.9	12
53	NIR II Luminescence Imaging for Sentinel Lymph Node and Enhanced Chemo-/Photothermal Therapy for Breast Cancer. Bioconjugate Chemistry, 2021, 32, 2117-2127.	1.8	12
54	Multifunctional LaPO ₄ :Ce/Tb@Au mesoporous microspheres: synthesis, luminescence and controllable light triggered drug release. RSC Advances, 2014, 4, 63425-63435.	1.7	11

RUICHAN LV

#	Article	IF	CITATIONS
55	Lanthanide-Based Nanocomposites for Photothermal Therapy under Near-Infrared Laser: Relationship between Light and Heat, Biostability, and Reaction Temperature. Langmuir, 2020, 36, 4033-4043.	1.6	11
56	Optimized Multimetal Sensitized Phosphor for Enhanced Red Up-Conversion Luminescence by Machine Learning. ACS Combinatorial Science, 2020, 22, 285-296.	3.8	11
57	A cheap and facile route to synthesize monodisperse magnetic nanocrystals and their application as MRI agents. Dalton Transactions, 2015, 44, 247-253.	1.6	9
58	Mesoporous semiconductors combined with up-conversion nanoparticles for enhanced photodynamic therapy under near infrared light. RSC Advances, 2019, 9, 17273-17280.	1.7	9
59	Plasmonic modulated upconversion fluorescence by adjustable distributed gold nanoparticles. Journal of Luminescence, 2020, 220, 116974.	1.5	9
60	A Magnified Adaptive Feature Pyramid Network for automatic microaneurysms detection. Computers in Biology and Medicine, 2021, 139, 105000.	3.9	9
61	An optimized lanthanide-chlorophyll nanocomposite for dual-modal imaging-guided surgery navigation and anti-cancer theranostics. Biomaterials Science, 2020, 8, 1270-1278.	2.6	8
62	Mesoporous NaYF ₄ :Yb,Er@Au–Pt(<scp>iv</scp>)-FA nanospheres for dual-modal imaging and synergistic photothermal/chemo-anti-cancer therapy. RSC Advances, 2015, 5, 43391-43401.	1.7	7
63	Synthesis, luminescence, and anti-tumor properties of MgSiO3:Eu-DOX-DPP-RGD hollow microspheres. Dalton Transactions, 2015, 44, 18585-18595.	1.6	5
64	Transferred Photothermal to Photodynamic Therapy Based on the Marriage of Ultrathin Titanium Carbide and Up-Conversion Nanoparticles. Langmuir, 2020, 36, 13060-13069.	1.6	5
65	Exosome-based rare earth nanoparticles for targeted <i>in situ</i> and metastatic tumor imaging with chemo-assisted immunotherapy. Biomaterials Science, 2022, 10, 744-752.	2.6	5
66	Early diagnosis and bioimaging of lung adenocarcinoma cells/organs based on spectroscopy machine learning. Journal of Innovative Optical Health Sciences, 2022, 15, .	0.5	5
67	Rare earth nanoparticles for sprayed and intravenous NIR II imaging and photodynamic therapy of tongue cancer. Nanoscale Advances, 2022, 4, 2224-2232.	2.2	4
68	Near-infrared light-induced imaging and targeted anti-cancer therapy based on a yolk/shell structure. RSC Advances, 2016, 6, 21590-21599.	1.7	3
69	Dual-molecular targeted NIR II probe with enhanced response for head and neck squamous cell carcinoma imaging. Nanotechnology, 2022, 33, 225101.	1.3	2
70	Gold Nanostars Combined with the Searched Antibody for Targeted Oral Squamous Cell Carcinoma Therapy. ACS Biomaterials Science and Engineering, 2022, 8, 2664-2675.	2.6	1
71	Lanthanide-semiconductor probes for precise imaging-guided phototherapy and immunotherapy. Journal of Bio-X Research, 2020, 3, 193-204.	0.3	0